Ergonomic optimization of rowing seats using personalized Human Body Models

Manuela Boin

Ulm University of Applied Sciences / Technische Hochschule Ulm

1 Abstract

Seat-related discomfort and health problems, which occur especially during long rowing tours or training sessions, can be reduced by rowing seats with a surface geometry that is ergonomically optimized for the particular rower. This seat optimization can be done by analyzing measured pressure distributions and modifying the standard seat surface geometry for a specific person based on these results using CAD tools. The project presented here focuses on the purely virtual development of the optimal geometry for specific rowers. FE simulations were performed using Human Body Models (HBMs) to define seat geometries for specific individuals.

Human body models were personalized using the scaling module of the PIPER toolbox, the ANSUR database and anthropometric measurements of male rowers of the Ulmer Ruderclub Donau e.V.. Metadata for THUMS 5 version 5.0.3 was developed for this virtual process. For the GHBM M50-0 version 4.5, publicly available metadata was used. A scaling procedure was defined and the results of the scaling process were compared for the two different baseline models.

Finally, these different personalized HBMs were used to define user-specific seats for the rowers through simulation. The resulting seat geometries were compared for different rowers.

2 Motivation

Sports equipment development and optimization needs to take into account physical and biomechanical requirements as well as safety. Special attention should be paid to the interaction between the equipment and the athlete. Differences in athlete anthropometry must be considered during development. The motivation for developing ergonomically optimized equipment includes optimizing performance in training and competition, avoiding overload and impairment of athletes, and improving comfort, especially during long periods of use. [1] In addition to optimizing equipment for large user groups, personalized equipment is widely used in sports, especially for elite athletes and, to some extent, for ambitious amateur athletes. Examples of ergonomically adapted sports equipment are bicycle or racing car seats, sports arches, sports or ski boots.

The presented study shows the ergonomic optimization of rowing seats for sculling. Sculling is characterized by fixed feet and a moving seat with load transfer from the buttocks to the seat by friction and form fit. While bicycle seats are often padded on the surface, rowing seats are made of wood or fiber-reinforced plastics and have rigid surfaces that cannot compensate for anthropometric differences. This motivates the ergonomic optimization of the geometrical surface of the seats.

A non-representative questionnaire conducted at the Ulmer Ruderclub Donau e.V. showed that 69% of participants reported health problems such as numbness in the buttocks or legs, burning or pins and needles, especially during long training sessions or rowing trips (Fig. 1). A second questionnaire with similar results was conducted with elite athletes of the German Rowing Association (Deutscher Ruder-verband e. V.).

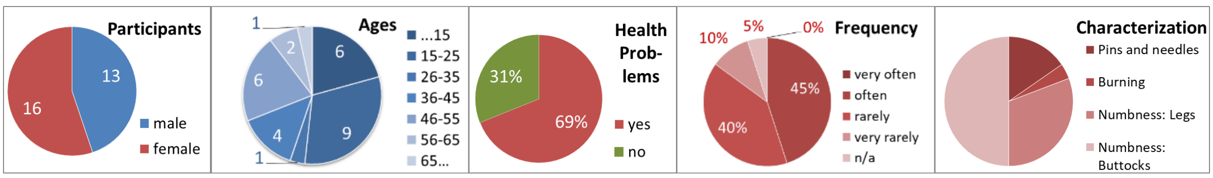

Fig.1: Results of a questionnaire done on 30.Jan.2017 in Ulmer Ruderclub Donau e. V. [2]

For elite athletes the main target for the application of optimized seats are long training sessions on the ergometer or in the boat, where health problems can occur. For amateur athletes the target are long rowing trips.

A previous study has already shown that the seat optimization can strongly reduce discomfort and health issues. A 79 day long rowing trip on the Danube from Ulm to the Black Sea (2583 km) was completed with about 5 hours of rowing per day without health problems caused by the seat. [2]

3 Methods

3.1 Comfort and discomfort of seats

The optimization of seat comfort is already part of the development process in the furniture, automotive and medical industries. While comfort is correlated with e.g. relaxation and well-being, discomfort is correlated with e.g. pain and numbness [3]. Several studies have shown that the discomfort of car seats can be evaluated by analyzing the pressure distribution between the seat and the seated person, the interface pressure. The pressure distribution should be smooth and as uniform as possible, with a low maximum pressure and a low gradient. [4], [5], [6]

Studies have also shown that seat (dis)comfort can be analyzed by simulation. This requires accurate models of the human body. Parameters that can be analyzed in the models include interface pressure, pressurized area, contact shear force, and load distribution within the body. [7], [8]

3.2 Overview of the virtual seat optimization process

The surface geometries of the rowing seats used on the aforementioned Danube tour were defined using design rules derived from a simulation pre-study, imprints defining the baseline geometry, and optimization cycles including CAD design, 3D printing of prototypes, and testing [2]. The project presented here focuses on the definition of the surface geometry of optimized rowing seats based on FE simulation using HBMs.

In order to define user-specific rowing seats by FE simulation, HBMs representing the specific user are required. Therefore, anthropometric measurements must be taken in the first step of the process. Based on these measurements, the HBM can be scaled in the second step. The third step is to define the reference for the interface pressure of this person using a standard rowing seat. In step 4, the surface geometry of the optimized seat is calculated and then used in step 5 to calculate the optimized interface pressure distribution. Figure 2 shows these five steps. Details of each step are given in the next two sections.

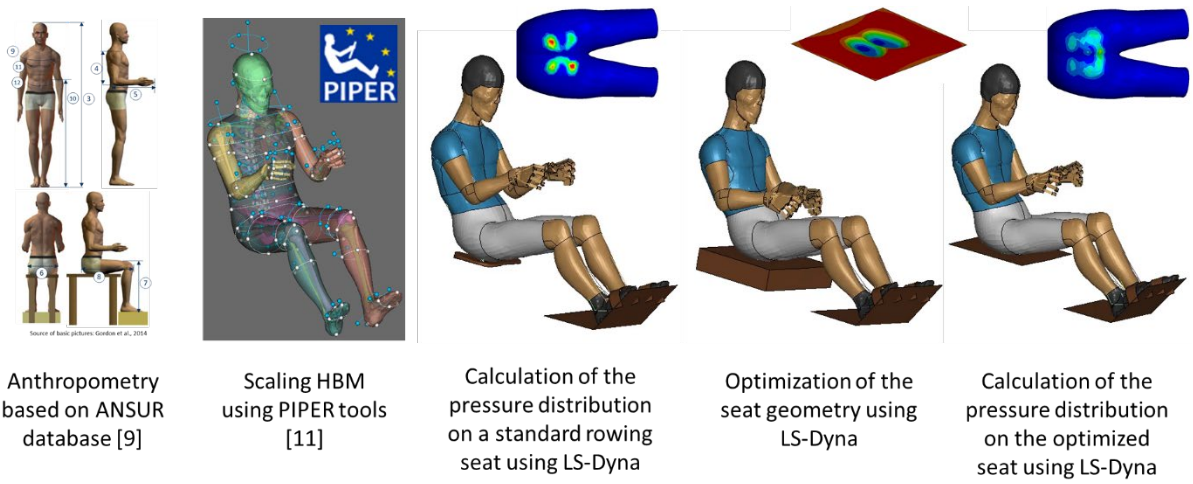

Fig.2: Overview of the five different steps in the seat optimization process [12]

4 Anthropometric measurements and scaling of the Human Body Models

4.1 Anthropometric measurements

Human body models are typically available in three different sizes representing a 5%ile, a 50%ile and a 95%ile of the base population. In most cases, these available models do not represent the target subjects. Therefore, it is necessary to scale the baseline models to the anthropometry of the specific rowers. The PIPER framework tools developed in the PIPER project [11] were chosen for the scaling of the HBMs. These tools allow for the definition of anthropometric targets using different databases: ANSUR [9], CCTAnthro [13], Snyder [14] and a GEBOD (Generator of Body Data) module [15]. The ANSUR database contains measurements of 1774 men and 2208 women of different ages who served in the US Army in 1988. Their average age was 25 years. The CCTAnthro database contains measurements from senior citizens, and the Snyder database contains measurements from children and adolescents.

Since all the target subjects of the project are adults, the ANSUR database is chosen for the target definition. The ANSUR database contains 132 direct and 60 derived measures. 12 representative measures and data were selected for the presented project. An overview of the selected data and the location of the length and circumference (circ) measures is given in Figure 3. These measurements were taken from different rowers. For the presented project, four male rowers were selected. These rowers are referred to as #0, #5, #7 and #8 based on the project listing. The Anthropometry module of PIPER was used to define targets for scaling the HBMs based on these individual measurements.

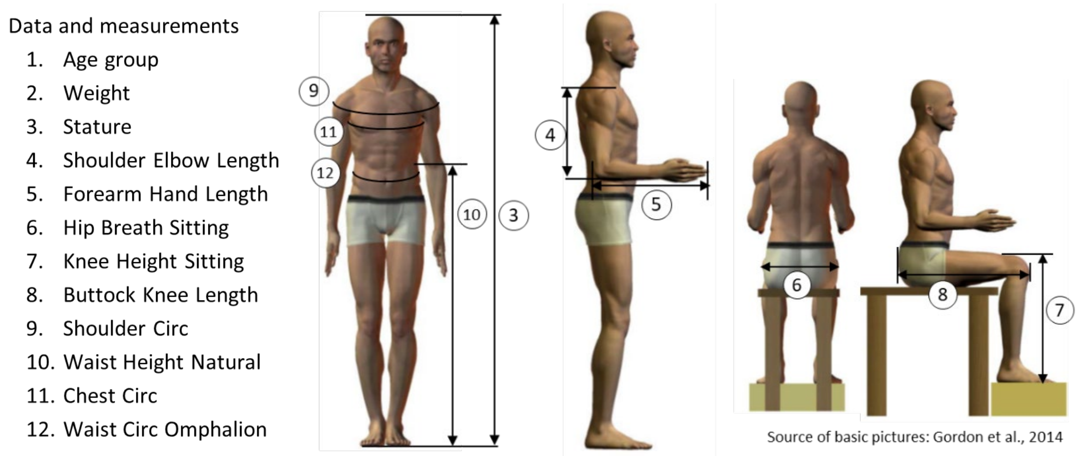

Fig.3: Overview of the measures used to define the anthropometric targets based on the ANSUR database [9], [10], [12]

4.2 Scaling of the Human Body Models

The target subjects of the project are four male rowers. Therefore, models of the 50% male were used for the study. In the first part of the project, the THUMS version 5.0.3 AM50 Occupant [16] was used as the baseline model. Since different HBMs are available, in the second part it was decided to test the developed methods on the GHBM M50-O 4.5 [17] and to compare the results for both widely used HBMs. The PIPER framework version 1.1.0 [18] was used for scaling.

The data transfer to the PIPER framework is done by metadata, which contains global information about the data format (solver format rules) and the HBM (unit system, height, weight, age), additionally anthropometric entities (e.g. skin and bone areas) and landmarks (e.g. top of the head) are defined. Depending on the anthropometric database used, the Simplified Scalable Model is defined. The format rules for reading LS-Dyna files and the metadata for the GHBM M50-O 4.5 have been created in the PIPER project. These are publicly available and could be used directly. [18]

The project required the development of metadata for scaling THUMS Version 5 AM50 with the Scaling Constraints module of PIPER. The anthropometric landmarks, skin and bone entities were defined and the Simplified Scalable Model was set up with the definitions of the segments and sections for scaling with the ANSUR database. Figure 4 shows the Simplified Scalable Model for THUMS with skin and bone entities on the left and landmarks, segments and sections on the right. [19]

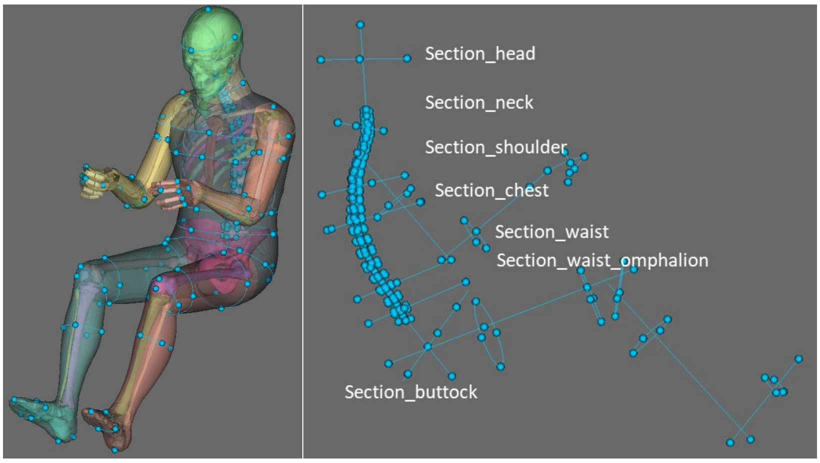

Fig.4: Simplified Scalable Model for THUMS 5 AM50 showing skin and bones entities on the left, and landmarks, segments and sections on the right [19]

In the Scaling Constraints module of PIPER, several parameters have to be set for the scaling process. These include the choice to use intermediate targets or not, the setting of thresholds for skin and bone entities, free or homogeneous decimation and the number of default nuggets. More detailed information can be found in the PIPER User Guide [11]. Different parameter settings were tested for the presented project [12]. For the THUMS model two different settings resulted in usable models. Both use two steps for the scaling process.

1. Homogeneous decimation, nuggets -100 and 0 thresholds for skin and bones followed by free decimation, nuggets 0 and 0 thresholds for skin and bones
2. Homogeneous decimation, nuggets -100 and 0 thresholds for skin and bones followed by the same again

Since the first parameter setting was not successful in scaling the GHBM, the second setting was used for the presented results.

4.3 Comparison of the targets and the scaled HBMs

Once the HBM has been successfully scaled, the quality of the personalization must be analyzed. This is done by comparing the measurements of the scaled model with the individual anthropometric targets.

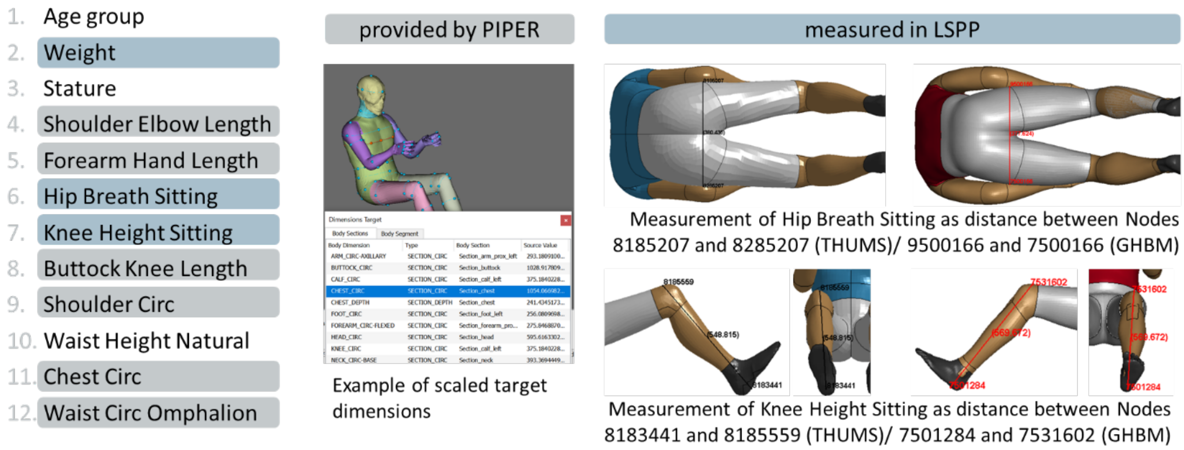

Fig.5: Overview of the measures used to compare the scaled models to the targets. Age Group, Stature and Waist Height Natural were used to define the targets, but could not be included in the comparison of the scaled models.

Some length and circumference measures of the scaled models, such as Shoulder Elbow Length and Shoulder Circ, are listed directly in PIPER. These measures are highlighted in light gray in Fig. 5. The values of Hip Breath Sitting and Knee Height Sitting need to be analyzed as node to node distances between appropriate nodes of the model using a standard pre-/post-processor such as LS-PrePost [20]. Since mass scaling is used in the HBMs, the correct weight of the scaled model must be taken from a short simulation run. Due to the slightly curved posture of the HBM, the multi-segment length measures Stature and Waist Height Natural are not available for the scaled models. Nevertheless, these measures as well as Age group were used for the target definition.

5 Seat optimization

5.1 Baseline model

The baseline model for the simulation of the interaction between the rowers and the seat consists of the HBM, the selected seat surface and the environment (see Fig. 2). The HBM is used in occupant position, since this position is very close to the mid-cycle position during rowing. No additional prepositioning of the HBM is done. The seat is modelled with a stiff, but deformable material model and is fixed at its bottom. It is positioned a short distance below the HBMs buttocks. The environment consists of plates in front of and under the feet and two straps to support the feet. The plates and straps are fixed at their edges. Loading by gravity is applied to the model. Surface to surface contacts with friction are defined.

In standard vehicle applications, the HBM is also supported by a backrest that provides a supporting load to the occupant. In rowing, there is no backrest. Therefore, this load is missing. Since the CoG of the HBM in occupant posture is positioned slightly behind the contact surface to the seat, a fully load/torque balanced condition is not achieved during the simulation. However, during the short simulation times the effect of the resulting upper body motion of the HBM on the results at the seat surface is small.

The parameters analyzed are the interface pressure between the buttocks and the seat and the pressurized area on the seat. To reduce the influence of the movement, the pressure distribution was analyzed as soon as the HBM completed the seating.

5.2 Seat optimization

The seat optimization is performed with the HBM in the static position of the base model. The dynamic rowing cycle is not yet included in the optimization. The seat of the baseline model is replaced by a block of deformable foam (40 x 50 x 10 cm³) covered by null shells (see Fig. 2). The foam is smoothly compressed by the weight of the HBM, creating an impression of the loaded buttocks. The stiffness of the foam is adjusted to achieve a maximum deformation of approximately 22 mm under the weight of the THUMS model. This preserves the typical depth of the surface geometry of rowing seats, which is necessary for form-fitting during the rowing cycle.

The null shells on the foam surface can then be used directly as the surface geometry of the optimized seat. Finally, the seat in the baseline model is replaced with the optimized geometry and the optimized interface pressure is calculated.

6 Results

6.1 Personalized Human Body Models

The personalization of the HBMs was done for four rowers with different anthropometry. Person #0 is about the same height as a 50%ile but much lighter, person #5 is taller and about the same weight, and person #7 and #8 were taller and heavier than a 50%ile. In addition, person #7 has long legs compared to the 50%ile and person #8 has a low measure of the waist circumference. All anthropometric measures of the four target subjects, the measures of the original HBMs and the measures of the scaled models for the different subjects are provided in Table 1. The left side shows the scaling results of the THUMS model and the right side shows the scaling results of the GHBM. Since some measurements were missing for subject #7, the average of the absolute values of the relative deviations of the scaled values from the target values was used as the overall evaluation criterion.

All scaled models show a reduction in the overall deviations from the anthropometric targets compared to the original models with the lowest overall deviations for the model of subject #5. The overall deviations range from 1,3% to 4,7% for the scaled THUMS models and from 1,1% to 2,9% for the scaled

GHBM. The highest deviations of single measures for the scaled THUMS models are found in the weight of the heavier subjects and in the small waist circ of subject #8. For the scaled GHBM the highest single measure differences are also found in the waist circ of subject #8 and in the weight of the lighter subjects. For the heavier subjects #7 and #8, the use of THUMS AM95 as a baseline model representing the taller and heavier part of the population could be investigated in the future.

Table 1: Anthropometric measures of the four target subjects, measures of the original HBMs, measures of the scaled models for the different subjects and relative deviations of the scaling results from the targets are shown. Left side: THUMS. Right side: GHBM.

Weight in 10^2g Length in mm	Age	Weight	Stature	Shoulder_Elbow_Length	Forearm-Hand_Length	Hip_Breath_Sitting	Knee_Ht_-_Sitting	Buttock_Knee_Length	Shoulder_Circ	Waist_Ht_natural	Chest_Circ	Waist_Circ-Omphalion	Average of absolute deviation	Average deviation for THUMS
THUMS 5.0.3 AM50		744	1750	360	509	380	549	636	1237		1054	933		
#0	24-30	670	1760	320	470	360	550	600	1120	900	920	810		
1.1.0_intermed_2x (-100, 0, 0)		661		330	473	361	525	599	1150		896	821		
Deviation from target		-1,3%		3,1%	0,7%	0,2%	-4,6%	-0,1%	2,7%		-2,6%	1,4%	1,9%	9,3%
#5	31-35	720	1920	400	520	345	590	550	1085	1070	990	820		
1.1.0_intermed_2x (-100, 0, 0)		706		405	521	339	565	551	1093		985	826		
Deviation from target		-2,0%		1,3%	0,1%	-1,6%	-4,3%	0,2%	0,7%		-0,5%	0,7%	1,3%	9,2%
#7	17-18	910	1960	370	550	380	620	770	1250					
1.1.0_intermed_2x (-100, 0, 0)		787		367	550	366	605	765	1256		997	885		
Deviation from target		-13,5%		-0,7%	0,0%	-3,6%	-2,5%	-0,6%	0,5%				3,1%	8,4%
#8	17-18	850	1860	390	490	380	570	630	1230	1080	1070	660		
1.1.0_intermed_2x (-100, 0, 0)		750		391	494	379	525	628	1247		1037	768		
Deviation from target		-11,8%		0,3%	0,9%	-0,2%	-7,9%	-0,4%	1,4%		-3,1%	16,4%	4,7%	8,0%

Weight in 10^2g Length in mm	Weight	Shoulder_Elbow_Length	Forearm-Hand_Length	Hip_Breath_Sitting	Knee_Ht_-_Sitting	Buttock_Knee_Length	Shoulder_Circ	Chest_Circ	Waist_Circ-Omphalion	Average of absolute deviation	Average deviation for GHBM
GHBM M50-O 4.5	779	384	489	378	570	587	1122	1014	862		
#0	670	320	470	360	550	600	1120	920	810		
1.1.0_intermed_2x (-100, 0, 0)	715	329	475	350	551	598	1105	919	785		
Deviation from target	6,8%	2,8%	1,1%	-2,8%	0,1%	-0,4%	-1,4%	-0,1%	-3,1%	2,1%	7,5%
#5	720	400	520	345	590	550	1085	990	820		
1.1.0_intermed_2x (-100, 0, 0)	759	406	522	339	588	550	1083	994	804		
Deviation from target	5,4%	1,5%	0,4%	-1,8%	-0,4%	0,0%	-0,2%	0,4%	-2,0%	1,3%	5,4%
#7	910	370	550	380	620	770	1250				
1.1.0_intermed_2x (-100, 0, 0)	881	370	552	379	631	766	1229	1016	845		
Deviation from target	-3,1%	0,0%	0,3%	-0,2%	1,8%	-0,6%	-1,7%			1,1%	10,3%
#8	850	390	490	380	570	630	1230	1070	660		
1.1.0_intermed_2x (-100, 0, 0)	820	393	495	383	549	627	1219	1045	740		
Deviation from target	-3,6%	0,8%	1,0%	0,8%	-3,7%	-0,5%	-0,9%	-2,3%	12,2%	2,9%	6,9%

The visual comparison of the two baseline models and the scaled models in Figure 6 shows that the individual anthropometry of the rowers could be obtained for both HBMs using the described scaling process. A more detailed comparison of the scaled models e.g. of the pelvic bones is provided in [12].

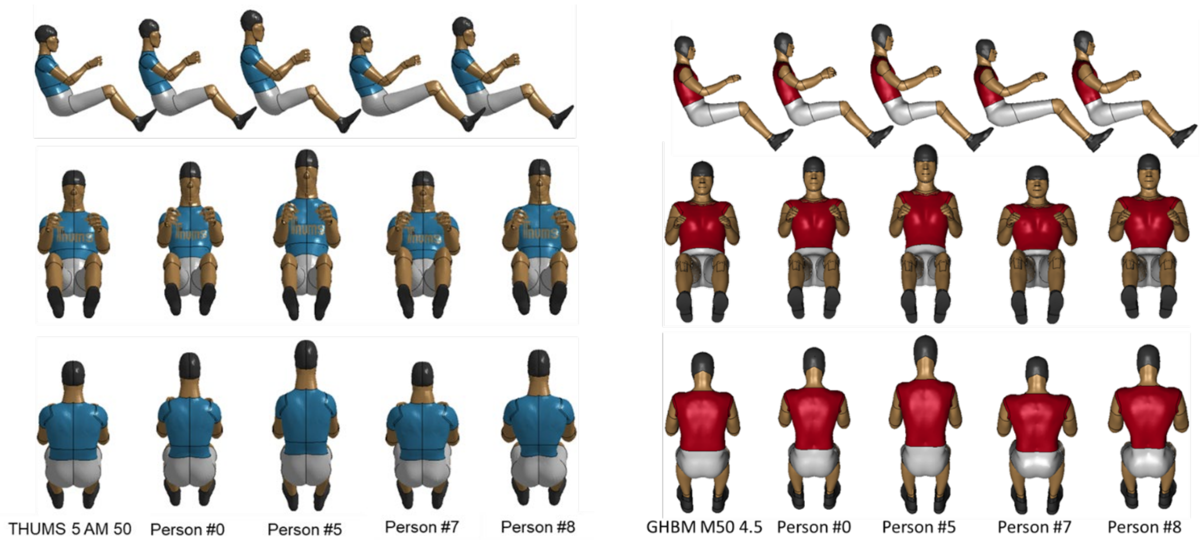

Fig.6: Side, front and rear view of the original HBMs and the scaled models. Left side: THUMS. Right side: GHBM.

All models were used in the following optimization process.

6.2 Interface pressure on the standard rowing seat

After successful scaling the models were placed on a standard rowing seat as described in 5.1 and the distribution of the interface pressure as well as the contact area between the HBM and the seat were analyzed. The top view of the seat used and its dimensions are shown in Fig. 7.

The interface pressure between the HBM and the seat (Fig. 8) shows a very localized distribution of high values. The maximum values of interface pressure for all models are found at the holes of the seat. For the GHBM models, high values also appear at the rear edge of the seat. The overall distribution is very localized for the THUMS models and more distributed for the GHBM. The contact area (pressurized/wetted area, Fig. 9) is very small for the THUMS models, but covers the seat for the GHBM.

Due to the larger contact area, the maximum pressure values for the GHBM are lower than for the corresponding THUMS model. However, the trends are the same: The highest interface pressures are found for model #5. Models #7 and #8 show the lowest interface pressures.

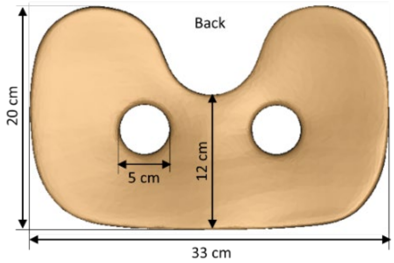

Fig.7: Top view and dimensions of the standard rowing seat.

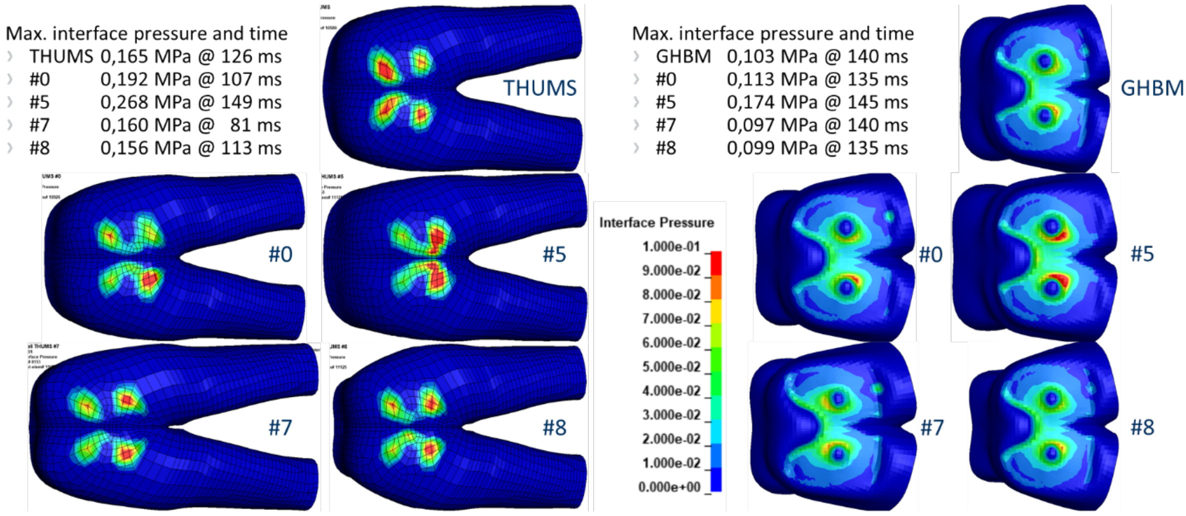

Fig.8: Distribution of the interface pressure at the buttocks for the different models on the standard rowing seat. All plots use the same scale from 0 MPa (blue) to 0,1 MPa (red). The back of the models is on the left. Left side: THUMS. Right side: GHBM.

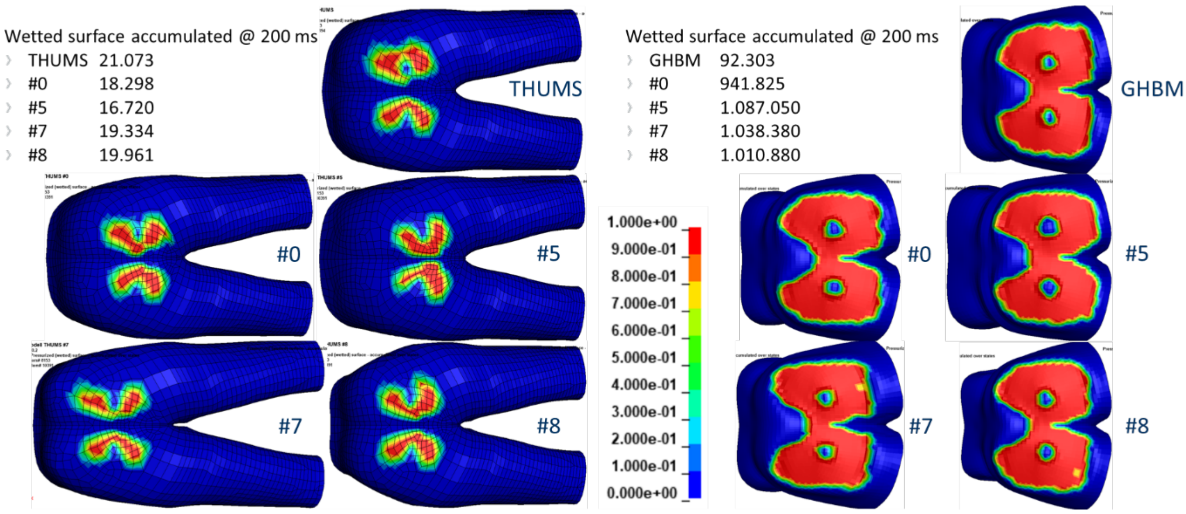

Fig.9: Distribution of buttock contact area to the standard rowing seat for the different models. All plots use the same scale from 0 (no contact, blue) to 1 (full contact, red). The back of the models is on the left. Left side: THUMS. Right side: GHBM.

The differences found in this analysis are based on the different levels of refinement of the HBMs used and the stiffness of the material models. While the THUMS version 5 AM50 is a simplified model, the GHBM M50-O is more detailed. The mesh size in the contact area ranges from 6 mm to 15 mm for

THUMS, with element areas between 70 mm² and 300 mm², and from 5 mm to 9 mm for GHBM, with areas of approximately 50 mm². The meshes of both models are shown on the left side of Figure 10. In addition, the material models of the two HBMs have different stiffnesses. The GHBM uses a softer model than the THUMS, which allows for more deformation under gravitational loading. The resulting differences in the deformation of the buttocks in contact with the rowing seat can be seen on the right side of Figure 10.

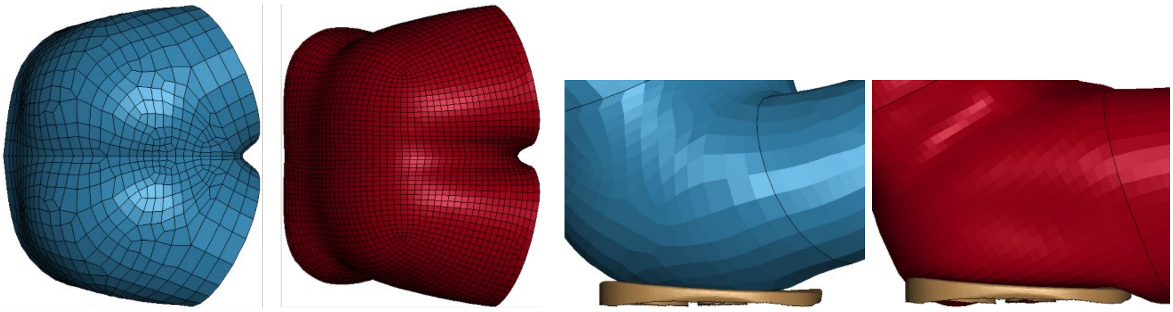

Fig.10: Detailed views of the buttock mesh and the deformation of the buttocks in the contact with the seat for the THUMS version 5.0.3 AM50 Occupant (blue) and the GHBM M50-O 4.5 (red).

The calculated maximum interface pressure values are used as a reference for comparing the optimized seat design.

6.3 Seat optimization

The optimization of the seat surface geometry is done as described in 5.2. Top and side views of the deformed foam surface for the different models are shown in Figure 11. The maximum deformation is also shown for each model. Due to the softer GHBM buttocks, the deformation is distributed over a larger area and the imprints are not as deep as for the THUMS models. However, the model with the largest deformation is #5 for both THUMS and GHBM.

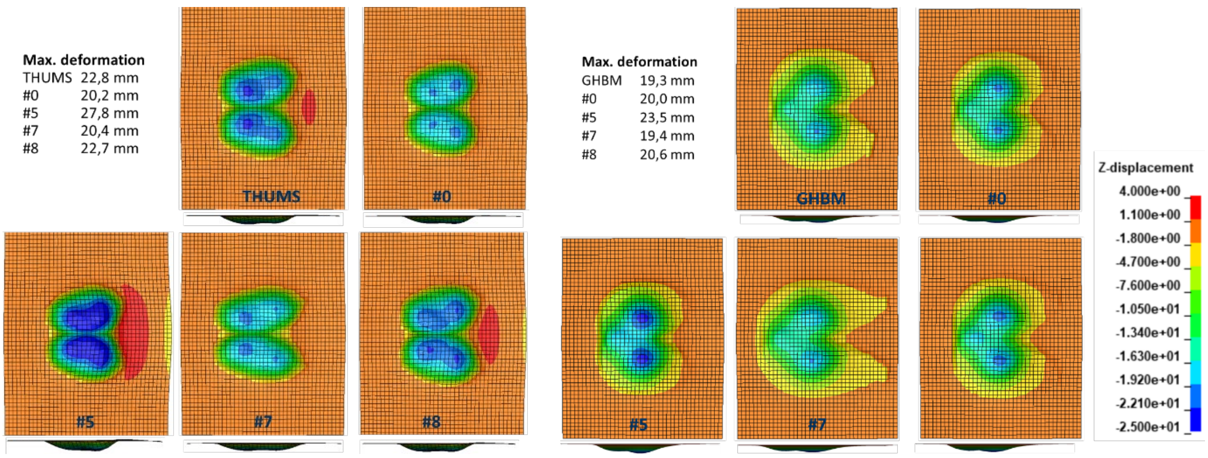

Fig.11: Top and side views of the deformation of the foam block under the gravitational load of the HBM. Negative z-displacements refer to compression. All plots use the same scale from -25 mm (blue) to +4 mm (red). The back of the HBMs is on the left. Left side: THUMS. Right side: GHBM.

The interface pressure on these personalized seat surfaces shows a significant reduction for all models (Fig. 12). Larger contact areas (Fig. 13) and smoother pressure distributions are found. The GHBMs still show larger contact areas and lower pressure values than the corresponding THUMS models, but an optimization was also found for these models.

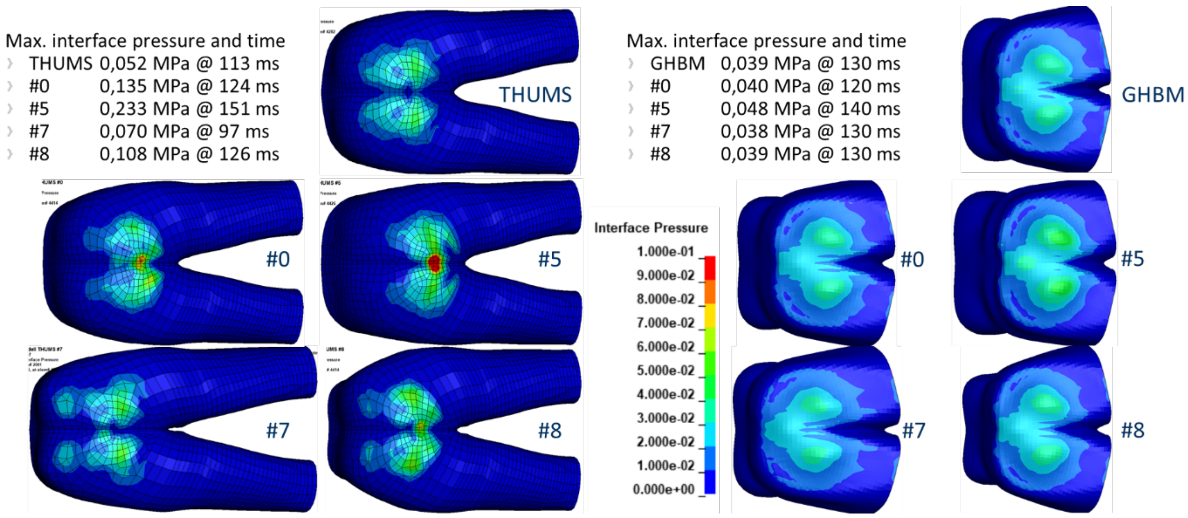

Fig.12: Distribution of the interface pressure at the buttocks for the different models on the personalized seats. All plots use the same scale from 0 MPa (blue) to 0,1 MPa (red). The back of the models is on the left. Left side: THUMS. Right side: GHBM.

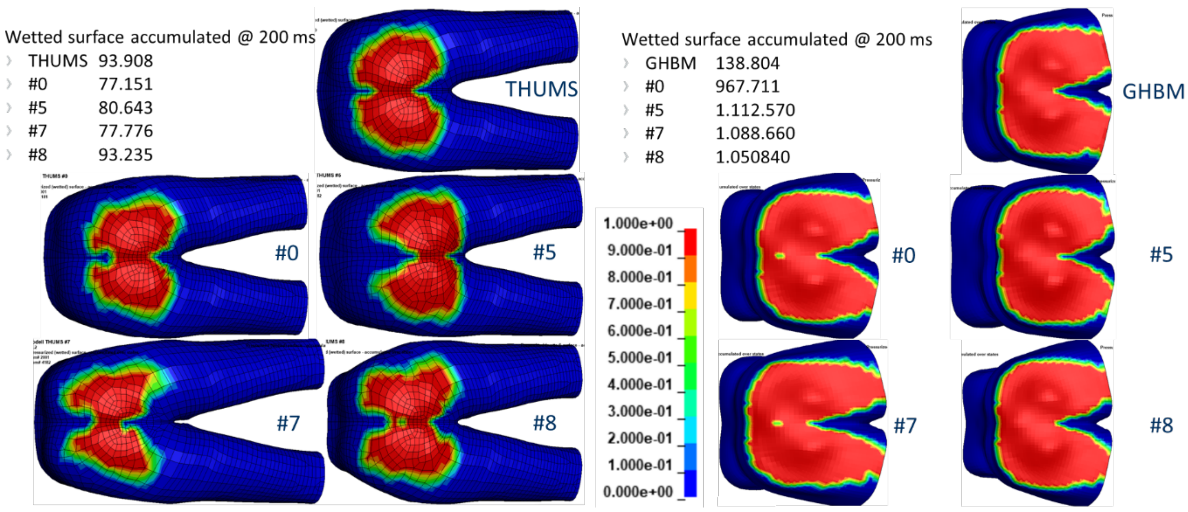

Fig.13: Distribution of buttock contact area to the personalized seat for the different models. All plots use the same scale from 0 (no contact, blue) to 1 (full contact, red). The back of the models is on the left. Left side: THUMS. Right side: GHBM.

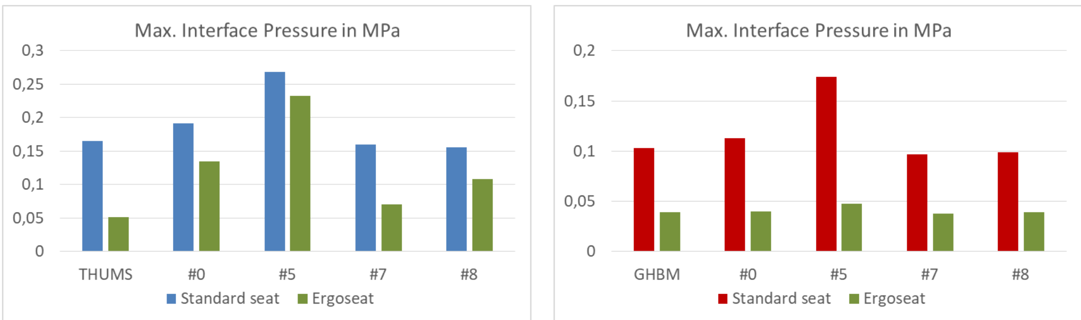

Fig.14: Comparison of maximum interface pressure for all models for the standard seat and the personalized seats. Left side: THUMS. Right side: GHBM.

The maximum interface pressure was reduced for all models using the optimized seat geometry (Fig. 14). Reductions ranging from 13% (THUMS #5) to 72% (GHBM #5) were achieved.

7 Summary

Metadata for the Scaling Constraints Module of PIPER has been set up for THUMS 5.0.3 AM50, including landmarks, segments, sections, skin and bone entities. Personalization of THUMS AM50 and GHBM M50-O was successfully performed on four different individuals using a workflow developed for the PIPER framework. The scaled models were compared. The selected anthropometries could be well reproduced with both baseline HBMs.

All original and scaled HBMs were used to analyze the interface pressure distribution and buttock contact area on a standard rowing seat. Pressure peaks due to the non-optimal seat surface were found. Personalized seat surfaces were created for each original and scaled HBM. The interface pressure distributions and contact areas were calculated for these optimized seats and compared to the corresponding models with the standard seat. The maximum interface pressure was significantly reduced for all models. The contact area between the buttocks and the seat was increased. Differences in the pressure distributions caused by the different anthropometry of the subjects could be reproduced. Systematic differences due to the different refinements and material models of the buttocks of the two different baseline HBMs were found.

The next steps in the project will be to compare the modeled interface pressure distributions with pressure measurements taken on different seats in a project with the German Rowing Association (Deutscher Ruderverband e. V.). This should provide more insight into the different modeling of the buttocks of the HBMs.

As mentioned in 5.2, the dynamic rowing cycle and the resulting load cycle of the seat is not yet included in the optimization. Adding this capability to the models will be an important step in the future of the project.

8 Literature

[1] Witte, K.: „Gesamtkonzept zur Entwicklung und Optimierung von Sportgeräten“, In: Sportgerätetechnik. Springer Vieweg, 2013, Berlin, Heidelberg. https://doi.org/10.1007/978-3-642-34702-3_7

[2] Boin, M.; Goebel, G.; Hofmann, H.; Hummel, S.: “Optimization of a Rowing Seat Using Human Modeling and 3D Printing Technology”, Conference on Human Modeling and Simulation in Automotive Engineering, Berlin, 2018, Oct 18-19

[3] Zhang, L.; Helander, M. G.; Drury, C. G.: “Identifying Factors of Comfort and Discomfort in Sitting”, In: Human Factors, Vol. 38, No. 3, 1996, pp. 377-389

[4] de Looze, M. P.; Kuijt-Evers, L. F. M.; van Dieën, J.: “Sitting comfort and discomfort and the relationships with objective measures”, In: Ergonomics 46 (10), 2003, S. 985–997

[5] Mergl, C.; Klendauer, M.; Mangen, C.; Bubb, H.: “Predicting Long Term Riding Comfort in Cars by Contact Forces Between Human and Seat”, In: 2005 Digital Human Modeling for Design and Engineering Symposium, 2005, Jun. 14

[6] Hartung, J.: „Objektivierung des statischen Sitzkomforts auf Fahrzeugsitzen durch die Kontaktkräfte zwischen Mensch und Sitz“, Dissertation am Lehrstuhl für Ergonomie, TU München, 2006

[7] Choi, H. Y.; Kim, K. M.; Han, J.; Sah, S.; Kim, S.; Hwang, S.; Lee, K. N.; Pyun, J.; Montmayeur, N.; Marca, C.; Haug, E.; Lee, I.: “Human Body Modeling for Riding Comfort Simulation”, In: Vincent G. Duffy (Hg.): Digital human modeling. First International Conference on Digital Human Modeling, ICDHM 2007, Beijing, China, 2007, July 22 - 27, pp. 813–823

[8] Grujicic, M.; Pandurangan, B.; Arakere, G.; Bell, W. C.; He, T.; Xie, X.: “Seat-cushion and soft-tissue material modeling and a finite element investigation of the seating comfort for passenger-vehicle occupants”, In: Materials & Design 30 (10), 2009, pp. 4273–4285

[9] Gordon, C. C.; Churchill, Th.; Clauser, Ch. E.; Bradtmiller, B.; McConville, J. T.; Tebbetts, I.; Walker R. A.: “1988 Anthropometric Survey of U.S. Army Personnel: Methods and Summary Statistics”, Technical Report NATICK/TR-89/044, 1989

[10] Gordon, C. C.; Blackwell, C. L.; Bradtmiller, B.; Parham, J. L.; Barrientos, P.; Paquette, St. P.: “2012 Anthropometric Survey of U.S. Army Personnel: Methods and Summary Statistics”, Final Report, Technical Report NATICK/TR-15/007, 2014

[11] PIPER Software Framework and Application: User guide; Version 1.0.1 – July 19, 2017, available at http://doc.piper-project.org/framework/1.0.1/user-guide.pdf

[12] Boin, M.: “Application of Personalized Human Body Models to the Optimization of Rowing Seats”, Conference on Human Modeling and Simulation in Automotive Engineering, Wiesbaden, 2022, Nov. 16-17

[13] CCTAnthro database: released under CC-BY-4.0 by CEESAR and distributed by PIPER, 2017

[14] Snyder, R.; Schneider, L.; Owings, C.; Reynolds, H.; Golomb, D.; M Schork, M.: “Anthropometry of infants, children, and youths to age 18 for product safety design”, Final Report, UM-HSRI-77-17, CPSC, Bethesda, MD, 1977

[15] Cheng, H.; Obergefell, L.; Rizer, A. (): “Generator of Body (GEBOD) Manual”, Final Report, AL/CF-TR-1994-0051 (ADA289721), 1994

[16] Toyota: Total HUman Model for Safety, available at https://www.toyota.co.jp/thums/

[17] GHBMC: Global Human Body Model, available at http://www.ghbmc.com/

[18] PIPER Project: PIPER Tools Framework, available at http://piper-project.org/framework

[19] Boin, M.; Döbler, N.: “Personalization of THUMS 5 (not only) for the optimization of rowing seats”, 8th International Symposium Human Modeling and Simulation in Automotive Engineering, 2020, Nov. 19-20

[20] DYNAmore: LS-PrePost, available at https://www.dynamore.de/en/products/pre-and-postprocessors/prepost